

APPLICATION OF THE TANGENT-STIFFNESS METHOD IN THE FINITE ELEMENT MODELLING OF THE BEHAVIOUR OF INTERFACE SURFACES

S.O. Edelugo

Department Of Mechanical Engineering, University Of Nigeria,
Nsukka, Nigeria, West Africa

PHONE: 2348037463298; e-mail: mcedeson@yahoo.com

ABSTRACT:

To simulate the behaviour of an interface formed between two contacting bodies using the finite element method, a review of previous approaches employed by other authors who worked with the same finite element method is carried out; their models and experimental data evaluated. A third-degree polynomial approximation approach is first undertaken to model the behaviour of the interface during loading, unloading and reloading. An incremental method and an iterative procedure are both employed. Finally, the tangent-stiffness method in which, for every iterative step, a portion of the external load is applied and the shear and normal stiffnesses are calculated is introduced. An example of a prismatic beam on a rigid base is analyzed and the predicted results are compared with those obtained from experiments.

Keywords: *Modeling; Interface-surfaces; Finite-element-method; Loading-reloading-unloading; Third-degree- polynomials; Tangent-stiffness-method.*

Symbols / Notations

a_i	area of contact of node I
A_{int}	apparent area of contact at the interface
a_1, a_2, a_3	coefficients of the - curve (loading branch)
a_{11}, a_{12}	slope and intercept of the straight lines obtained when a_1, a_2, a_3 are plotted against pressure
a_{21}, a_{21}	
a_{31}, a_{32}	
b_0	distance of the unloading branch of the - curve from the original
b_1, b_2, b_3	coefficients of the - curve (loading branch)
b_{11}, b_{12}	slope and intercept of the straight lines obtained when b_1, b_2, b_3 are plotted against pressure
b_{21}, b_{21}	
b_{31}, b_{32}	
c	constant determined by the characteristic of the interface an defined by equation (1)
c_0	distance of the reloading branch of the - curve from the origin
c_1, c_2, c_3	coefficients of the - curve (reloading branches)
c_{11}, c_{12}	slope of and intercept of the straight lines obtained when

c_{21}, c_{22}	c_1, c_2, c_3 are plotted against pressure
c_{21}, c_{22}	
d_1	deflections of the interface element i
e	number of elements to which node i is common
e_1	number of elements in the contacting bodies
e_2	number of interface elements
E	equivalent Young's modulus of the contacting bodies
F_z	normal load acting on the structure
F_{zj}	incremental load acting on the structure during the j th iteration in the z -direction
F_{zj}^i	normal force acting on beam i after the j th
$\{F_{xb}, F_{yb}, \dots, F_{sb}\}$	forces acting on beam i
k_n	normal stiffness of the interface
k_{nj}	normal stiffness of beam i for the j th iteration
k_{sx}	shear stiffness in the x -direction
k_{sy}	shear stiffness in the y -direction
k_{int}	stiffness matrix of an interface element
k_b	stiffness matrix of an element representing the contacting bodies
k_s	structural stiffness matrix
m	constant determined by the characteristic of the surface
P	pressure at the interface
P_{av}	average interface pressure resulting from a uniform distribution of the first incremental load F_{z1}
P_j^i	pressure in beam i after the j th iteration
u_p, v_j, \dots, w_2	deflections of the nodes of an interface beam in the x -, y -, and z -directions
l	normal deflection at the interface
l_1	normal deflection in beam i due to force F_{zj}^i
t	shear stress at the interface
t_j	limiting value of shear stress due to friction
t_l	shear stress in the beam after the iteration in which the limiting value of shear stress is exceeded
t	shear stress in the beam after the first re-analysis

1. INTRODUCTION

When structures are analyzed by numerical methods, it is sometimes acceptable to ignore the influence of joints formed by the constitutive elements of a structure. In the analysis of interface surfaces in machine tools, however, they cannot be ignored because their flexibility can account for a fairly large percentage of the deflection

occurring at the cutting edge [1].

In the case of bolted joints the stiffness depends upon the bolt preload, the geometry of the flanges and bolt, the area over which the bolt load is applied and the characteristics (i.e. the surface roughness, hardness, machining methods employed, etc.) of the mating surface. Several research workers [2-7] have considered the geometry of the joint

and developed empirical relationships for the stiffness of the assembly and for the pressure distribution along the interface. Some of these relationships are based upon the pressure cone theory.

The advent of large-scale computers and the rapid growth of the finite element method have made it possible to obtain more accurate models. Cullimore and Eckart [8] extended an earlier empirical relationship [9] to cater for a three-bolt three-flange assembly. Fernlund [10] assuming that a single plate can replace two plates estimated the contact pressure and area but Gould and Mikic [11] using an iterative finite element technique have shown that the assumptions made in [10] could lead to serious errors. Thompson *et al* [12] using an experimental/finite element approach found that the contact area is independent of the bolt preload and bolthole diameter. In another paper, Jofiert *et al* [13] developed from finite element studies empirical relationships for the interface pressure and contact area for ring-loaded flanges. Schafer [14], Mahtab and Goodman [15] extended the finite element model by introducing bond elements between the contacting bodies and modeled the behaviour of the joint in shear.

The above models do not take into account the characteristics of the contacting surfaces.

Back *et al* [16] represented the normal stiffness of the interface by using beam and plate-like elements. However, their model caters only for the situation when the interface or part of it is being continuously loaded. The model developed herein calculates the stiffness of the interface when it is being loaded, unloaded or reloaded. The model also takes into account

the shear stiffness of the interface. The tangent-stiffness method [17] is used to calculate these stiffness values and it is shown that this method gives results that are more accurate than those obtained by the method employed in [16].

2. NORMAL AND SHEAR BEHAVIOUR OF AN INTERFACE

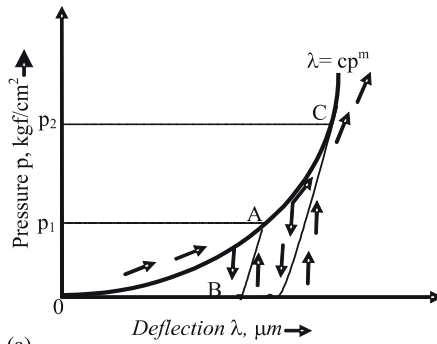
Several research workers have studied deflections experimentally [1,18,19]. Briefly, when two specimens are brought into contact and a load normal to the interface is applied, the deflections produced lie on the curve OA (Fig. 1a). If the loading is stopped, for example at pressure p_1 , and then gradually decreased, the unloading curve, AB, is almost linear and corresponds to the elastic behaviour of the specimens. If the load is increased again, the behaviour is elastic until the pressure, p_2 is reached after which the deflection follows the curve OAC again until the next unloading cycle. It has been found [1] that the curve OAC can be adequately described by the following equation:

$$= cp^m \quad \dots(1)$$

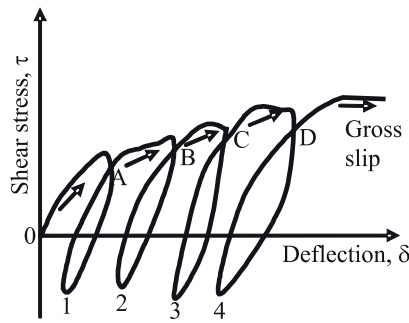
Where δ is the deflection at the interface, p is the pressure and c and m are constants determined by the characteristics of the interface.

In addition to normal loads, shear loads may act upon the joint. The behaviour of an interface loaded in shear has been studied,, amongst others ,by Kirsanova [20], Masuko [21] and Sanad [22]. A typical shear deflection curve for an interface is shown in Fig. 1b. This curve, which is obtained with a constant normal pressure and varying shear load acting on the interface, can be divided into three parts:

- (a) The loading curve formed by the segments OA, AB, BC, etc
- (b) The unload branches A1, B2, C3, etc.;
- (c) The reload branches 1A, 2B, etc.



(a)



(b)

Fig . 1. Normal and shear behaviour of an interface

Unlike the pressure-deflection curve, there is no known simple equation to represent the shear stress-deflection curves. It was decided to use polynomials to represent each part of the curve. Several tests were conducted and it was found [23] that a third-degree polynomial of the type:

$$t = a_1d + a_2d^2 + a_3d^3 \quad \dots (2)$$

represented the loading curve accurately. The term a_0 is absent because the curve passes through the origin.

The unload branches are disjointed because they start from different points on the main curve. They have, however, the same shape. This was verified by translating

the different branches so that they passed through the same point (i.e. the origin). Notice the resulting interloop. This important property made it possible to group them together and represent them by a single third-degree polynomial:

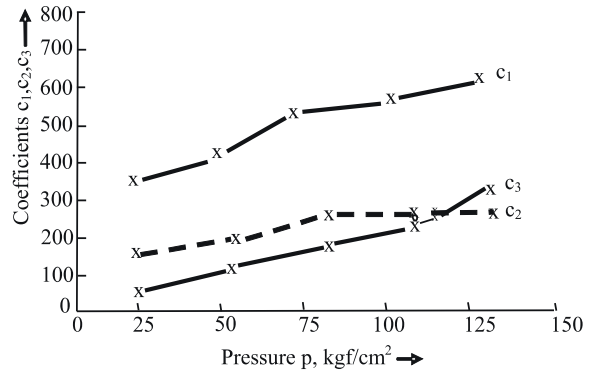
$$t = b_1d + b_2d^2 + b_3d^3 \quad \dots(3a)$$

Each branch has to be uniquely identified and this is done by expanding the above equation and including the term b_0 ; whose value is made equal to the amount by which the branch has to be translated so that it passes through the origin.

Therefore, for unloading:

$$t = b_0 + b_1d + b_2d^2 + b_3d^3 \quad \dots(3b)$$

Fig. 2 Approximation of the pressure-deflection curve



It was found that an identical procedure could be used for the reloading branches and the polynomial to represent them is:

$$t = c_0 + c_1d + c_2d^2 + c_3d^3 \quad \dots(4)$$

The behaviour of the interface shown in fig. 1b is for a specific value of normal pressure. If the normal pressure is changed, another but a similar $t - d$ curve is obtained. For example, from the experimental results obtained, by Sanad [22] for ground mild steel, the reloading branches at different normal pressures, when translated to pass through the original, were approximated at follows:

$$\begin{aligned}
 p &= 24 \text{ kgf/cm}^2; t = 337.99d - 116.34d^2 + 26.76d^3 \\
 p &= 50 \text{ kgf/cm}^2; t = 427.52d - 115.45d^2 + 90.50d^3 \\
 p &= 75 \text{ kgf/cm}^2; t = 609.50d - 264.80d^2 + 166.34d^3 \\
 p &= 103 \text{ kgf/cm}^2; t = 647.83d - 280.89d^2 + 265.61d^3 \\
 p &= 128 \text{ kgf/cm}^2; t = 724.83d - 276.43d^2 + 361.66d^3
 \end{aligned}$$

Figure 2 shows the values of the coefficients of d , d^2 , d^3 plotted against the normal pressure. The maximum value of p considered is 128 kgf/mm^2 because this was the maximum pressure, which the experimental rig, designed and built by Sanad [22], could exert on the test specimens. Assuming that at higher normal pressure a similar trend is exhibited, the values of c_1 , c_2 and c_3 (in equation 4) can be approximated to vary linearly with p . Thus, in equation form: $c_1 = c_{11} + c_{1p}$, $c_2 = c_{21} + c_{22p}$ and $c_3 = c_{31} + c_{32p}$. If these values are substituted into equation (4) and the term c_0 is neglected because its value is associated with a particular branch, a general equation to represent the reloading branches is obtained:

$$t = (c_{11} + c_{12p})d + (c_{21} + c_{22p})d^2 + (c_{31} + c_{32p})d^3 \dots (5)$$

For the load and unload branches, a similar linear variation of the coefficients with normal pressure was observed. Therefore, equation (2) and (3a) can be re-written as:

$$t = (a_{11} + a_{12p})d + (a_{21} + a_{22p})d^2 + (a_{31} + a_{32p})d^3 \dots (6)$$

and

$$t = (b_{11} + b_{12p})d + (b_{21} + b_{22p})d^2 + (b_{31} + b_{32p})d^3 \dots (7)$$

3. STIFFNESS MATRIX OF AN INTERFACE ELEMENT

To model the above non-linear behaviour, beam elements are introduced between the two contacting bodies. For the three-dimensional case, each interface node has three degrees of freedom: two (u, v) in the plane of the joint and one normal to it (w). The force-deflection relationship for an interface element, I , is given below:

$$\begin{Bmatrix} \Delta F_{x1} \\ \Delta F_{y1} \\ \Delta F_{z1} \\ \Delta F_{x2} \\ \Delta F_{y2} \\ \Delta F_{z2} \end{Bmatrix}_i = \begin{bmatrix} k_{sx} & 0 & 0 & -k_{ax} & 0 & 0 \\ 0 & k_{sy} & 0 & 0 & -k_{sy} & 0 \\ 0 & 0 & k_n & 0 & 0 & -k_n \\ -k_{sx} & 0 & 0 & k_{sx} & 0 & 0 \\ 0 & -k_{sy} & 0 & 0 & k_{sy} & 0 \\ 0 & 0 & -k_n & 0 & 0 & k_n \end{bmatrix} \begin{Bmatrix} u_1 \\ v_1 \\ w_1 \\ u_2 \\ v_2 \\ w_2 \end{Bmatrix}$$

$$\{DF\}_I = (k_{int})\{d\}_i \dots (8)$$

Note that l is given by $(w_1 - w_2)$ and the shear deflection, d , by $(u_1 - u_2)$ or $(v_1 - v_2)$. Although the shear and normal stiffnesses appear to be uncoupled, it was shown earlier [equations (5-7)] that the shear stiffness is dependent upon the normal pressure. In the calculations below, the normal and shear forces DF_{z1} (or $-DF_{z2}$), DF_{x1} (or $-DF_{x2}$) and F_{y1} (or $-DF_{y2}$) are designated by DF_z^i , $Dand$ DF_y^i respectively. The suffix, hereafter, refers to the iteration number.

4. DETERMINATION OF THE NORMAL AND SHEAR STIFFNESS

The most commonly used methods to model non-linear behaviour are the step-wise, iterative and mixed methods. In the iterative method, the structure is fully loaded in each iteration and the portion of the load that is not equilibrated is used in the next step to compute an additional increment of deflection.

This process is repeated until the deviation from equilibrium becomes negligible. Back *et al* [16] used a modified version of this technique to model the pressure-deflection curve. The convergent curve obtained by them was oscillatory in nature; the oscillations were damped out by averaging two consecutive sets of results.

In the step-wise method, which has been used herein, the total load applied to the system is subdivided into several partial

loads which need not be of equal magnitude. During each iteration the relationship between the forces and displacements is assumed to be linear. This relationship, i.e. the stiffness matrix as defined by equation (8), can be evaluated using either the ‘secant modulus’ or the ‘tangent-stiffness’ method. A description of these methods is given in [17]. In the first iteration, the former is used; in the second and subsequent iterations the latter is used. The accumulated values of the increments of displacement corresponding to the force increments, gives the total displacement for the intended load. Given below is a detailed description of how these methods have been adapted to calculate the normal and shear stiffnesses of the interface when it is being loaded, unloaded or reloaded.

4.1 Normal stiffness during loading

The process starts by subdividing the total external load F_z into several load increments. For the first iteration, it is assumed that the actual area of contact is equal to the apparent area of contact, A_{int} . Therefore, for the iteration, the incremental load, DF_{z1} , is distributed over the entire interface.

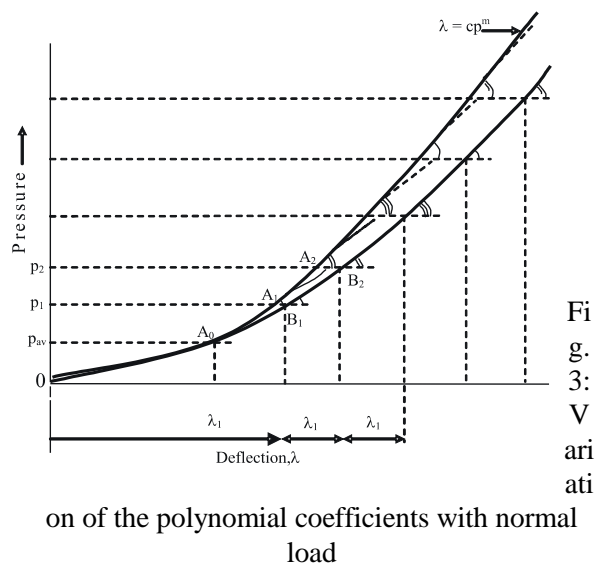
To calculate the force acting at an interface node, it is necessary to know (i) the pressure at the node and (ii) the area, a_i , over which it exerts an influence.

For the first iteration, it is assumed that DF_{z1} will cause a uniform pressure, p_{av} , across the interface therefore its magnitude is given by DF_{z1}/A_{int} . The area of influence, a_i , ascribed to an interface node i can be shown equal to $S^e \iint N_i dx dy$ where e is the number of elements the node is common to. This derivation is based upon the assumption that the pressure remains constant over the element. It was found that the variation in the pressure had to be one degree lower than that assumed for the displacement functions. The

stiffness matrices of the elements in the contacting bodies were derived using linear shape functions. When a linear variation of pressure was tried with these elements incorrect pressure distribution were obtained. For example, in an axisymmetric problem, instead of the pressure maintaining a constant value around the circumference of a given circle, it oscillated. Note that the sum of all the areas of influence is equal to A_{int} and that the above expression merely helps to subdivide A_{int} into region. Therefore, for the first iteration the load acting at node i is

$$DF_z^i = p_{av} \cdot a_i$$

This concentrated force acting at the node will cause the asperities within its area of influence to deform. This deformation can be calculated from equation (1) and is represented by the deflection, l_ϕ^i , occurring in the beam which is introduced at node i : $l_0^i = c \cdot p_{av}^m$. Hence the normal stiffness at this point on the interface is:



$$k_{nl}^i = \frac{\Delta F_{z1}^i}{\lambda_0^i} = \frac{P_{av} a_i}{C P_{av}^m} = \left(\frac{\Delta F_{vl}}{A_{int}} \right)^{1-m} \cdot \frac{a_i}{C}$$

This value corresponds to the slope of the line OA₀ in Fig.3 For this first iteration; one cannot use the slope of the curve because its value is zero at the origin.

The value of the normal stiffness as given by equation (9) is now used in equation (8) to calculate the stiffness matrix for the interface element. The above procedure is repeated for all the interface elements. These matrices are now combined with the stiffness matrices of the elements representing the contacting bodies to form the global stiffness matrix of the structure:

$$[k_s]_1 = \sum^{e1} [k_b] + \sum^{e2} [k_{int}]_1$$

A finite element analysis of the structure is now performed with the first incremental load DF_{z1} acting on it. From the resulting displacements, the relative deflection between the two ends of beam i can be extracted. Let this be represented by λ₁ⁱ. This pressure acting at the same node after the first iteration can now be calculated:

$$p_1^i = \text{element force} / \text{area of influence} \\ = \text{Stiffness} \times \text{deflection} \\ = \frac{k_{nl}^i \cdot \lambda_1^i}{a_1}$$

This value of pressure is now intersected with the curve to locate point A₁ (fig.3). The slope of the curve at this point is required to calculate the stiffness of the beam element i for the second iteration. Differentiating equation (1) gives the slope of the curve at a point:

$$\frac{dp}{d\lambda} = \frac{p^{1-m}}{m \cdot c}$$

Since, k_n = (dp/dl)_{a_i} the normal stiffness of

the interface node i for the second iteration

$$\text{is: } k_{n2}^i = \left(\frac{dp}{d\lambda} \right)_{AI} \cdot a_1 = \frac{(p_1^i)^{1-m} \cdot a_1}{m \cdot c}$$

The interface element stiffness matrices are recalculated with the new values of k_n. Matrices [k_b] are not recalculated because the deflections occurring in the structure are small and its behaviour is elastic. Therefore:

$$[k_s]_2 = \sum^{e1} [k_b] + \sum^{e2} [k_{int}]_2$$

The second incremental load, DF_{z2}, is applied and another finite element analysis is performed. This causes deflection, λ₂ⁱ, to occur in element i and from it the pressure p₂ⁱ in the beam at the end of the second iteration can be calculated [equation (10)]:

$$p_2^i = \frac{k_{n2}^i (\lambda_2^i + \lambda_1^i)}{a_i} \dots (10)$$

The normal stiffness for the third iteration is:

$$k_{n3}^i = \frac{(p_2^i)^{1-m} a_i}{m \cdot c} \dots (11)$$

This process is repeated until all the incremental loads have been applied. The final deflection of the interface at node i is given by λⁱ = λ₁ⁱ + λ₂ⁱ + ... + λ_kⁱ where k is the number of iteration performed.

The pressure calculated from equation (13) is assumed to act over the part of the interface, which is assigned to node i. Over this region it is assumed to be constant. There is, however, with this model a discontinuity in the pressures occurring in adjacent regions. This discontinuity will decrease as the number of nodes in the finite element model is increased.

The magnitude of the incremental

forces, DF_{zk} , are arranged to be either in a geometric or an arithmetic progression. This seems justifiable considering the exponential nature of equation (1). Since the value of k_n for the first iteration is calculated using the secant OA_0 , the first iteration load is F_{z1} is chosen to be small (about 5 per cent of the total load). The greater the initial load, the greater is the magnitude of A_1B_1 (fig. 3) which is the error incurred in the first iteration.

4.2 Normal stiffness during unloading and reloading

As the total load is increased, the pressure in the regions around the load also increases. At the same time, in the other regions the pressure decreases thus initiating the unloading process. As mentioned earlier, during unloading the joint behaves as if the two bodies were rigidly connected. This results in curve AB (fig. 1a) that can be approximated to a straight line; its slope is given by the equivalent Young’s modulus of the contacting bodies.

If, during the iterations, a beam is found to go into tension, it indicates that unloading has begun. For the next iteration, its stiffness is:

$$k_n^i = \frac{dp}{d\lambda} \cdot a_1 = E \cdot a_i$$

This value is used as long as the beam continues to be unloading. When the sum of the incremental forces acting on it becomes zero, the beam is removed from the finite element model. This indicates that a certain amount of area at the interface has lost contact. The deflection occurring in the beam when it is disconnected represents a permanent deflection, l_B (fig. 1a) which has occurred at the interface.

In subsequent iteration, due to a change in loading conditions, the same regions of the interface may begin to approach each other. When the relative deflection between a contact nodepair reaches l_B (fig. 1a) the beam is reintroduced. This indicates that this part of the interface has been brought into contact and reloading has begun. The stiffness of the beam is calculated from the slope of the reloading curve BA. When the deflection in the element reaches the value corresponding to point A, an equation similar to (14) is used once again to calculate the normal stiffness of the interface element.

4.3 Calculation of the shear stiffness

The shear stiffness, k_{sx} and k_{sy} , are calculated using the stepwise method. The total force, as before is applied in increments. For all the iterations, including the first, the shear stiffness of a beam is calculated using the tangent-stiffness method

$$\begin{aligned} k_s &= \frac{\text{shear force}}{\text{shear deflection}} \\ &= \frac{\text{shear stress} \times \text{area of influence}}{\text{shear deflection}} \\ &= \left(\frac{\tau}{\delta} \right) a_i \end{aligned}$$

The value of τ/δ is evaluated from the slope, dt/dd , of the loading, unloading or reloading curve. If equation (6) is used, the shear stiffness of beam i is:

$$\begin{aligned} k_s^i &= (dt/d\delta) \cdot a_1 \\ &= (a_1 + 2a_2d + 3a_3d^2) \cdot a_i \end{aligned}$$

where $a_1 = (a_{11} + a_{12} p_1)$, etc. This equation is used for all the iterations. Note that for the first iteration, the slope of the curve at the origin is used and therefore

$$k_{s1}^i = (d\tau/d\delta)_{origin} = a_1 \cdot a_1$$

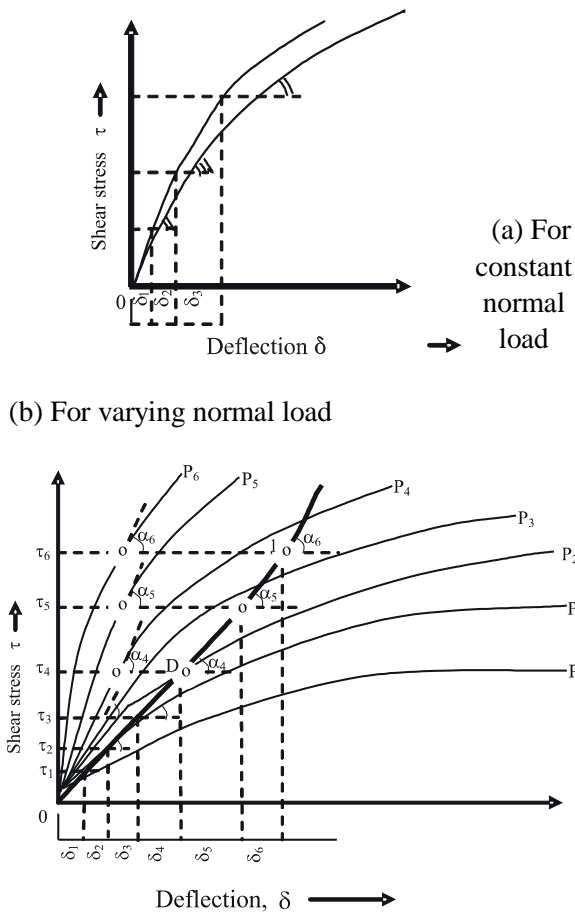


Fig. 4 Approximation of the t-d curve

For the second and subsequent iterations, the cumulative of the incremental shear deflections is used to locate the point on the curve at which the tangent is drawn. Therefore, for example, for the third iteration

$$\delta = \delta_1^i + \delta_2^i \quad \delta_1^i \quad \text{wh} \delta_2^i \quad \text{and} \quad \text{are the}$$

shear deflections occurring in the beam in the

first and second iterations.

Figure 4a shows how the loading curve is approximated by lines OA, AB, etc.: their slopes are the same as the tangent to the curves. This approximation is valid only if the normal pressure remains constant. If an increase in the shear force results in a corresponding increase in the normal pressure, as would happen if the plane of the joint is not normal to the direction of application of the load, a different curve has to be used for each iteration. The shear behaviour of the interface is now approximated by OA, AB, BC, etc. (fig. 4b) whose slopes, a_1, a_2, a_3 , etc., are obtained from the curves, P_0, P_1, P_2, P_3 , etc. These curves represent the shear behaviour of the interface at different normal pressures.

4.4 Coefficient of friction

The model also takes into consideration the coefficient of friction. By limiting the maximum shear force that can be transmitted through the joint, the coefficient of friction defines the position (point D, Fig. 5a) at which the loading curve stops and slip begins to occur. The curve OPQ should be represented by the tangents OA, AB, BC, CD and DE. DE represents the small amount of slip, which is permitted to occur in localized regions in the vicinity of the bolt load. With the tangent stiffness method, it is difficult to model the transition from CD to DE. Consider the situation at the interface where one of the beams after k iterations has deflected d_k (fig. 5a), for the next iteration, the shear stiffness of the beam is calculated from the slope of the curve at point P.

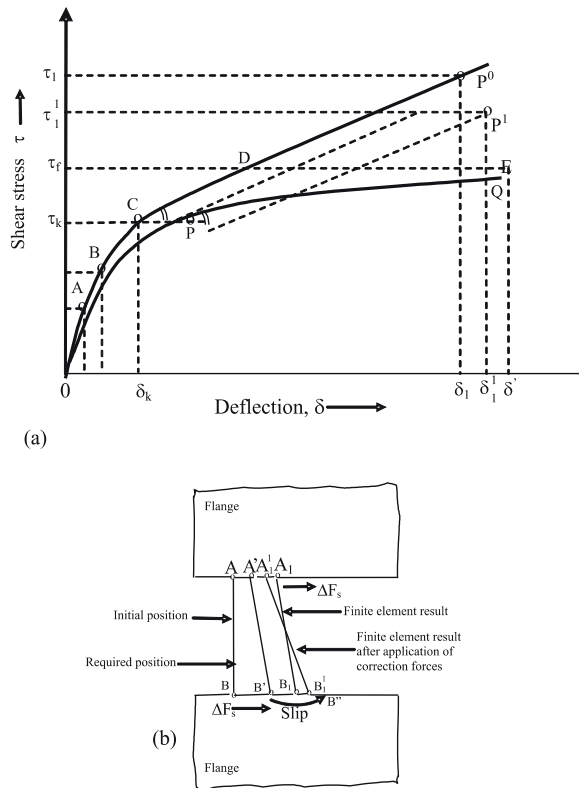


Fig. 5. Modeling the - near the limit of friction

At the end of this iteration, the shear acting at this beam is t_1 which exceeds the limiting value t_f but the resulting deflection, d_k . This is also illustrated in Fig. 5b. AB represents the initial position of the beam. The beam should deflect to A 'B' with B'B'' representing the slip. However, the finite element model moves the beam to position A_1B_1 . The sole reason for considering the coefficient of friction is to reduce the excess stress ($t_1 - t_f$) and to correct the position of A_1B_1 . It is not intended to model the behaviour of the joint when gross-slip occurs; for this the reader is referred to [24,25]. To reduce the excess stress, an approach suggested in [26] has been adapted herein. The excess force, whose magnitude is given by $(t_1 - t_f)$, is applied at the interface nodes after which the structure is re-analysed. The

beam AB under the action of the correcting force DF_s (fig. 5b) now deflects to positions $A_1^1 B_1^1$, which is nearer to the required position A'B''. After the first re-analysis, the excess shear stress is reduced to $(t_1^1 - t_f)$. It is suggested in [26] that the model is re-analysed several times until the excess

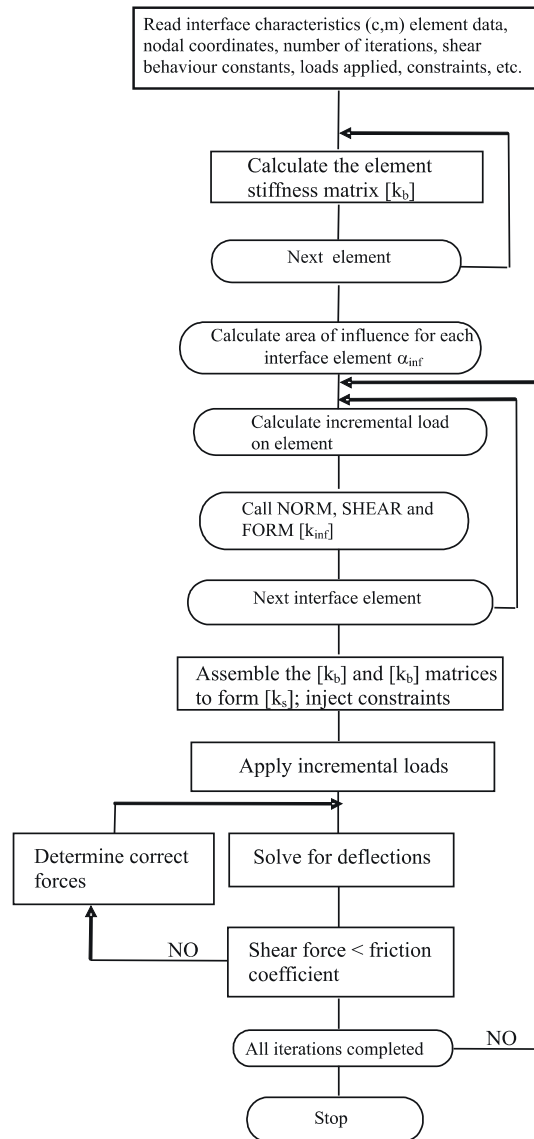


Fig. 6a Flow diagram for solving contact problems

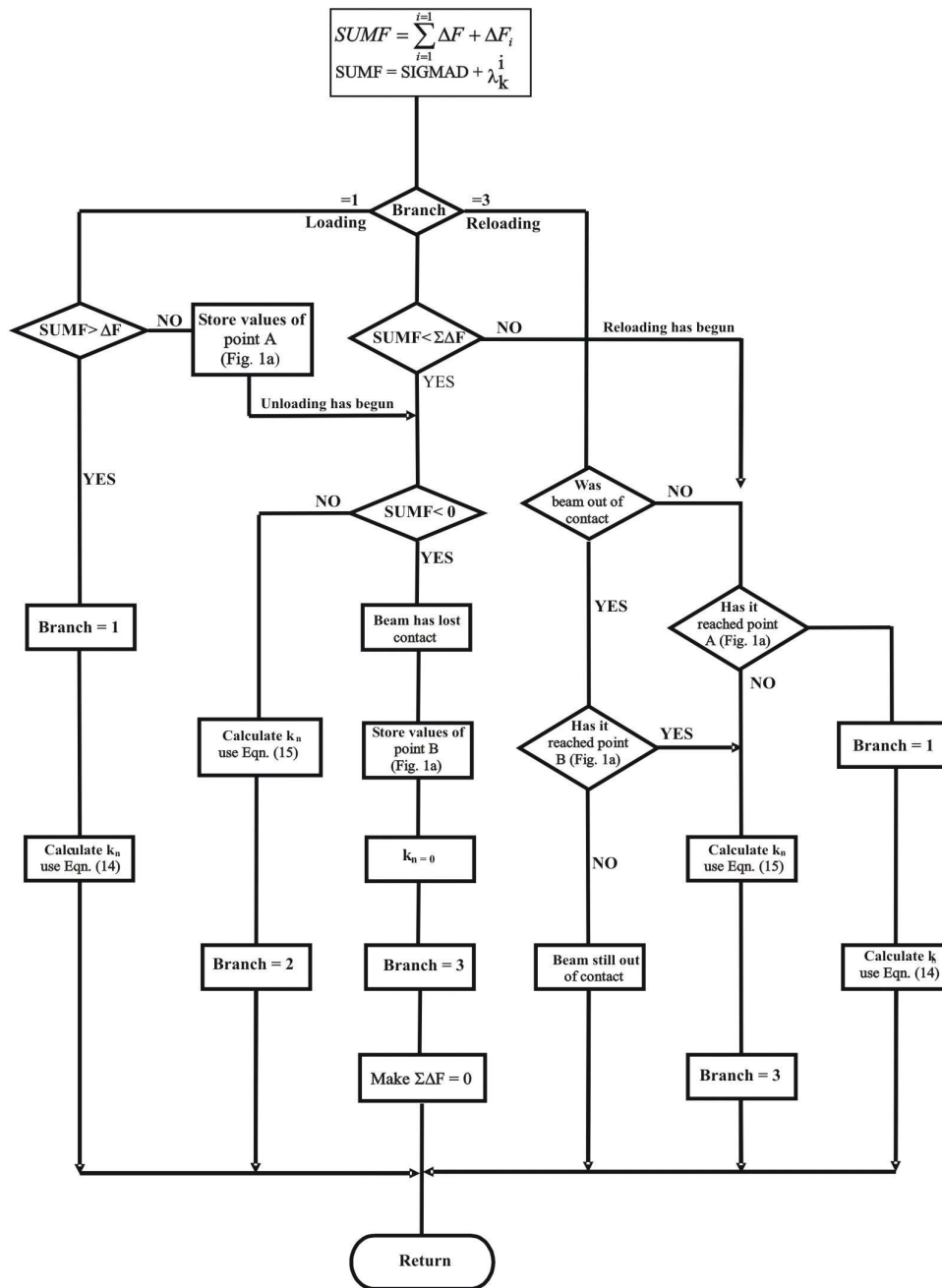


Fig. 6b Flow diagram for subroutine SHEAR

shear stress become zero. This was found to be very expensive with respect to computing time because several re-analysis are required for every node where slip has just occurred. Because of this and the fact that the shear behaviour of the interface plays a secondary

part in the case of fixed joints, it was decided to perform only one re-analysis. It was found that this reduced the excess stress by 60 per cent.

5. COMPUTATIONAL PROCEDURE

The overall operation is described by the

flowchart shown in Fig. 6a. In addition to the data required to describe the finite element model such as nodal coordinates, element node numbers, the user must supply the values of c and m , the number of iterations required, the coefficients which describe the t - d curve, and the manner in which the external load is to be divided into incremental loads.

To start with, the program calculates the stiffness matrices of the elements representing the contacting bodies. For the interface elements, the values of k_n and k_s are calculated by subroutines NORM and SHEAR. The flowchart for NORM is shown in Fig. 6b. For the first iteration, the calculation of k_n is straightforward. For the second and subsequent iterations, the values of BRANCH, SUMF and SIGMAF are examined to decide which part of the pressure-deflection curve should be used to calculate k_n . Note that SUMF and SIGMAF, the current and previous sums of the incremental forces sustained by the beam are given by the following expressions:

$$SIGMAF = \Delta F_{z1}^i + \dots + \Delta F_{z(k-1)}^i$$

$$SUMF = SIGMAF + \Delta F_{zk}^i$$

where k is the iteration which has just been completed.

A similar but more complex procedure is used in SHEAR to calculate the value of k_s . In a three-dimensional problem, two calls are made to this subroutine because the shear stiffness in the plane of the joint may not be equal.

After each iteration is completed, the shear force sustained by a beam is compared with the limiting friction force; if it exceeds the latter, correction forces are calculated and included in the overall load vector. A re-analysis is performed before passing on to the next iteration.

6. RESULTS AND DISCUSSION

6.1 Prismatic beam on a rigid base

The example to be analysed is a simple rectangular prism (Fig. 7 inset) which lies with one of its longitudinal narrow faces against a plate of infinite stiffness. An external load is applied at mid-length and compresses the prism against the rigid base. The prism is represented by in-plane rectangular elements and the interface by beam elements (not shown in the inset, Fig. 7). The rigid base is simulated by fixing one end of the beams. Because the problem is symmetrical, suitable constraints are imposed on nodes which lie on the center-line and only one-half of the structure is analysed.

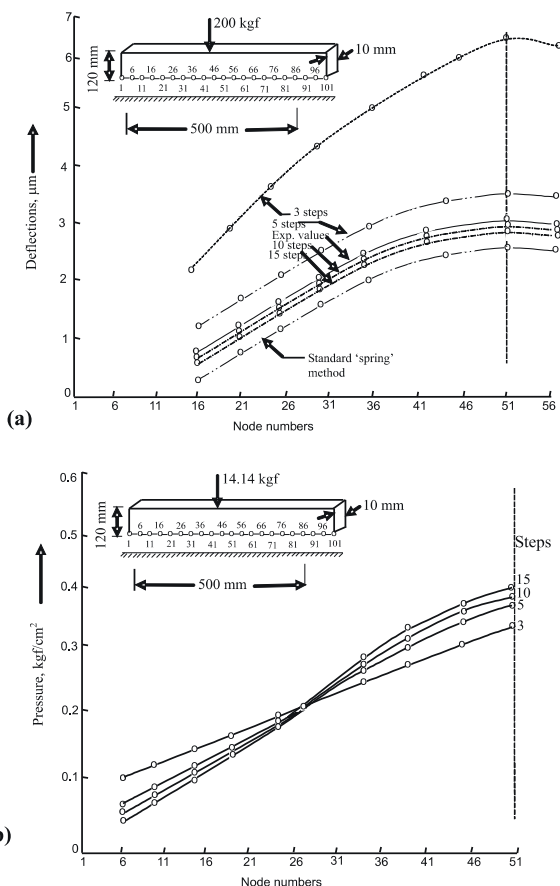
This example was selected for two reasons: experimental values of the interface deflections are available from Levina [28] and it has also been analysed by Back *et al* [16] using a 'standard spring' method. These two sets of results serve as a basis of comparison. Levina and Back *et al* did not consider the shear stiffness of the interface, and therefore the finite element results shown in Fig. 7 take into account only the normal stiffness of the interface. In general, the interface deflection is given by the compression occurring in a beam element. Since, in this example, one end of each beam is constrained, the interface deflection is given directly by the *downward* deflection of the nodes lying on the interface i.e. nodes labeled 1,6,11,16, etc. in Fig 7a. Figure 7b shows the pressure at each of the interface nodes.

With the incremental method, the accuracy obtained depends upon the number of steps chosen by the user. This problem has been analysed with three, five, ten and fifteen steps.

Increasing the steps from three to five results in a relatively large increase in the accuracy of the predicted results; the increase in the accuracy from ten to fifteen steps is only marginal and does not justify the extra computing effort. For this problem, Levina quotes a value of $c = 0.8 \text{ mm}$ and $m = 0.5$ and modulus of elasticity of 9500 kgf/mm^2 . The results obtained by the incremental method converge to a value slightly higher than the experimental results. The results obtained by the method suggested in [16] are even further removed from the experimental values.

Fig. 7 Interface pressure and deflections for a plate on a rigid base

Another important observation is that if



the convergence curve were to be plotted for the interface deflection at node 51, it would be monotonic in nature and would converge

from 'above'. However, in the case of pressure (Fig.7b), the nature of the convergent curve depends upon the position of the node along the interface. For example, the pressure for nodes 36 to 51 converges from 'below', whereas for nodes 6, 11, 16, 21 and 26 it converges from 'above'.

7. CONCLUSIONS

The tangent-stiffness method has been adapted to model the normal and shear behaviour of an interface. It was found that the loading, unloading and reloading branches of the t-d curve could be approximated by third-degree polynomials. The results are fairly accurate if the load is subdivided into five or more partial loads. The model has yielded results which agree with the experimental values.

REFERENCES

1. Restov, D. N. and Levina, Z. M. *Machine design for contact stiffness*. Machines and Tooling, 1965, vol. 36, No. 12, pp 15-23.
2. Roetscher, F. *Die Maschinenelement*, Springer Verlag, Berlin, 1927.
3. Little, R.E. Bolted joints: how much gives? *Machine Design*, 1967, No. 9, pp 173-175.
4. Boenick, U. Untersuchungen an Schraubenverbindungen. Dissertation, T. U. Berlin, 1966.
5. Motosh, N. *Determination of joint stiffness in bolted connections*. *Trans. ASME*, vol. 54 Aug. 1976, pp 858-861.
6. Zukov, V. B. *Calculating the elasticity of components in a bolted joint*. *Russian Engng. J.*, 1968, p48.
7. Dubrovskii, A. F. Determination of the load factor in designing bolted joints. *Russian Engng. J.*, 1967, 47, 46-47.
8. Cullimore, M. S. G. and Eckhart, J. B. *The distribution of the clamping pressure in friction-grip bolted joints*. *The structural Engineer*, 1974, vol. 52, No. 4, pp 129-131.

9. Cullimore, M. S. G. and Upton K. A. *The distribution of pressure between two flat plates bolted together*. Int. J. Mech. Sci., 1964, vol. 6, pp 13-25.
10. Ferlund, I. A. *Method to calculate the pressure between bolted or riveted plates*. Konstruktion, 1970, vol. 22, No. 6, pp 218-224.
11. Gould, H.H. and Mikic, B. B. *Areas of contact and pressure distribution in bolted joints*. Trans ASME, Aug. 1972, vol. 63, pp 864-880.
12. Thompson, J. C., Sze, Y. Strevel, D. G. and Jofriet, J. C. *The interface boundary conditions for bolted flanged connections*. J. Pressure Vessel Technology, 1976, vol. 34, pp 277-282.
13. Jofiert, J.C., Sze, Y. and Thompson, J.C. *Further studies of the interface conditions for bolted flanged connections*. Trans. ASME. 1981, vol.,103, pp 240-245.
14. Schaefer, H. *A contribution to the solution of contact problems*. Comp. Meth. App. Mech. Engng., 1975, vol. 6, pp 335-354
15. Mahtab, M. A. and Goodman, R. E. *Three dimensional finite element analysis of jointed rock slopes*. Proc. 2nd Conf. of int. Soc. Rock Mech., 1970.
16. Back, N., Burdekin, M. and Cowley, A. *Pressure distribution and deformations of machine components in contact*. Int. J. Mech. Sci., 1973, vol 15 pp 993-1010.
17. Desia, C. S. and Abel, J. F. *Introduction to the finite element method*, Van Nostrand-Reinhold, 1972.
18. Connolly, R. and Thornley, R. H. *The significance of joints on the overall deflection of machine tool structures*. Proc. 6th MTDR conf., 1965, pp 139-156.
19. Ostrovskii, V. I. *The influence of machining tools on slideway contact stiffness*, Machines and Tooling, 1965, vol. 36, No. 1, pp 17-19.
20. Kirsanova, V. N. *The shear compliance of flat joints*. Machines and Tooling, 1967, vol. 3, No. 7. pp 671-789
21. Masuko, M., Ito, Y. and Fujimoto, C. *Behaviour on horizontal stiffness and the micro-sliding on the bolted joint under preload*. Proc. 12th MTDR Conf., 1971, pp 81-88.
22. Sanad, F. H. *Performance of joints used in machine tool construction with particular reference to their stiffness and damping capacity*. PhD thesis, University of Manchester, 1981.
23. Villanueva-Leal, A. *The modeling of characteristics of interface surface by the finite element method*. PhD thesis, University of Manchester, 1980.
24. Fredriksson, B. *Finite element solution of surface nonlinearities in structural mechanics with special emphasis to contact and fracture mechanics problem*. J. of Computers and Structures, 1976, vol. 6, pp 281-290.
25. Okamoto, N. and Nakazawa, M. *Finite element incremental contact analysis with various frictional conditions*. Int. J. Num. Meth Engng., 1979, vol.14, pp 337-357.
26. Vallippan, S. *Stress analysis of rock as 'no tension' material*. Geotechnique, 1968, 18, 56-66.
27. Hinduja, S. *The application of the finite element method to machine tool structures*. PhD thesis, University of Manchester, 1971.
28. Levina, Z. M. *Calculation of contact deformation on slideways*. J. of Machines and Tooling, 1965, vol. 36, No.1, pp 567-956
29. Tsutumi, M., Ito, Y. and Masuko, M. *Deformation mechanism of bolted joint in machine tools*. Bull. Japan Soc. Mech. Engrs., 1979, vol. 22,, pp168-892.
30. Dolbey, M. and Bell, R. *The contact stiffness of joints at low apparent interface pressures*. Annals of C.I.R.P., 1971, pp 67-79.
- 31 Willner K., *Elasto-plastic Normal Contact of Three- Dimensional Fractal Surfaces Using Half-space Theory*. ASME Journal of Tribology. Jan. 2004, vol. 126, 1 Issue1, pp28-33

- 32 Marshal, M.B., Lewis, R., & Dwyer-Joyce, R. S., *Characterization of Contact Pressure Distribution in Bolted Joints*, Journal of Strain, Feb., 2006. Vol 42, issue 1, pp 31-43
- 33 David F., & Jason DeJong *Discrete Element Modeling of Solid-solid Interface Behaviour*. PhD Thesis: Manuel Recalde, Engineering Computer Science Institute, University of Buffalo, SURF,2000 Fellow.
- 34 Narasinha Rao., Krishnar Kumar, Bohara P. C. & Moakhopadhyey, R. A *Finite Element Algorithm for the Prediction of Steady-state Temperatures of Rolling Tires*. Tire Science & Technology Journal.Sept., 2006, vol. 34, issue 3, pp195-214.
35. Lihua You, etal *Finite Difference Surface Representation Considering Effect of Boundary Curvature*. *Geometric Modeling: Techniques, applications, systems and tools*. Kluwer Academic Publishers, 2004, Norwell, M.A.
36. Wingo, etal, *Hardware assisted self-collision for rigid and deformable surfaces*, Journal of Tele-operators and Virtual Environments. Dec., 2004. Vol. 13, No 6 pp 681-691
37. Brian Von Herzen, etal. *Geometric Collisions for Time- dependent parametric surfaces*. ACM SIGGRAPH Computer Graphics, Aug., 1990. Vol. 24, No. 4 pp 39-48
38. Neil Molino, etal. *A Virtual Algorithm for Changing Mesh Topology During Simulation of Contact Surfaces*. ACM Transactions on Graphics (TOG). Aug., 2004, vol. 23, No 32.